Journal of Applied Electrochemistry **31**: 663–670, 2001.

Effects of Zn and Pb as alloying elements on the electrochemical behaviour of brass in borate solutions

K.M. ISMAIL, S.S. EL-EGAMY and M. ABDELFATAH
Chemistry Department, Faculty of Science, Cairo University, Giza, Egypt

Received 19 September 2000; accepted in revised form 28 November 2000

Key words: borate, brass, Cl^- ions, EIS, Pb, polarization

Abstract

The electrochemical behaviour of brasses with various Zn content (5.5–38) and brass (Cu–38Zn) with different Pb content (1.3–3.3) in borate solution, pH 9.0, was investigated. The effects of applied potential and the presence of aggressive Cl^- ions were also studied. Different electrochemical methods such as open-circuit potential measurements, polarization techniques and electrochemical impedence spectroscopy (EIS) were used. Increase in zinc content decreases the corrosion rate of brass in borate solution exponentially. Long immersion of leaded brasses and alloys with different Zn content improves their stability due to the formation of a passive film. The passive film formation under open-circuit and potentiostatic conditions proceeds via dissolution–precipitation mechanism. The addition of a low concentration of Cl^- ion (0.01 M) to the borate solution increases the corrosion rate of Cu–38Zn due to dezincification. Increase in Cl^- ion concentration (0.01–0.2 M) decreases the corrosion rate of the brass exponentially due to formation of insoluble CuCl. For Cl^- ion concentrations >0.2 M the corrosion rate of the brass increases again due to the formation of the soluble $CuCl_2^-$ complex.

1. Introduction

The electrochemical behaviour of brasses (Cu–Zn alloys) has been extensively studied under different experimental conditions using various measurement methods including chemical, electrochemical, radiometric, spectro-electrochemical and surface techniques [1–15]. Most of the reported studies are directed to the dezincification process of the different types of brasses [3–10]. When dezincification occurs, regions of the brass become replaced by a porous mass of copper which has no strength.

Little work has been reported concerning the effect of a systematic increase of zinc content or minor alloying elements (such as Al, As, Sn or Pb) on the electrochemical behaviour of brass alloys [11, 12, 16]. The addition of small amounts of Al or Sn (~1–2%) to Cu–Zn alloys was found to improve the alloy corrosion resistance in sea water [16]. This effect has been attributed to the change in the microstructure, the number of defects, the segregation of the alloy and properties or composition of the passive film. Also the addition of small amounts of Pb (~1–3.2%) to Cu–Zn alloys has been found to increase the corrosion resistance of brasses in acidic and neutral chloride and sulphate media [11, 12]. Addition of about 0.04% arsenic was reported to inhibit dezincification of α-brasses in most circumstances. Additions of antimony or phosphorus, in amounts similar to arsenic, are claimed to be also capable of preventing dezincification of α-brasses [17].

Borate solution (3% $Na_2B_4O_7 \cdot H_2O$) is used as coolant in closed recirculating systems, especially in road vehicles. Moreover, alkaline borate is employed in boiler feed-water of power plants to inhibit pipe corrosion [17]. The present work is an investigation of the electrochemical behaviour of a variety of brasses in borate solution intended to clarify the mechanism of the corrosion and passivation processes taking place at the electrode–electrolyte interface in borate solution. The electrochemical behaviour of Cu–Zn alloys with 5.5, 24 and 38% Zn was studied. The effect of addition of Pb on the electrochemical behaviour of the Cu–38Zn alloy was investigated. The effects of applied potential and the presence of aggressive Cl^- ions on the behaviour of the Cu–38Zn alloy were also studied. Different electrochemical techniques (e.g., open-circuit potential measurements, polarization techniques and electrochemical impedance spectroscopy (EIS)) were used.

2. Experimental details

The working electrodes were made from brass rods, mounted into glass tubes by two-component epoxy resin leaving a surface area of 0.2 cm^2 to contact the solution. The material used were commercial-grade brass of different zinc contents, Cu–5.5Zn and Cu–24Zn were of the α-phase, whereas Cu–38Zn was of the (α + β)-phase [18]. Three leaded brasses, Cu–38Zn, containing

1.4, 2.7 and 3.3Pb were also used. The cell was a three-electrode all-glass cell, with a platinum counter electrode and saturated calomel reference electrode. Before each experiment, the working electrode was polished mechanically using successive grades of emery paper up to 1000 grit. Electrochemical measurements were carried out in borate–boric acid buffer (0.1 M $Na_2B_4O_7$ + 0.1 M H_3BO_3, pH 9.0) and in the same buffer solution containing NaCl (0.01–0.6 M).

The electrochemical impedance investigations and polarization measurements were performed using the Zalner Elektrik IM5d system. The potentials were referred to the saturated calomel electrode (SCE). All cyclic voltammetry measurements were carried out using a scan rate 10 mV s^{-1}. For the calculation of the corrosion current, i_{corr}, and corrosion potential, E_{corr}, the potentiodynamic measurements were conducted at a scan rate 1 mV s^{-1}. Details of the experimental procedures are described elsewhere [11, 12, 19].

3. Results and discussion

3.1. *Effect of Zn as alloying element*

It is well known that copper and zinc together form a wide series of solid solutions [18]. The addition of zinc to copper offers mechanical properties superior to those of copper. The corrosion resistance of brass varies widely based on the surrounding environment.

3.1.1. *Open circuit potential measurements*

Open-circuit potentials of brasses with different Zn contents (5.5, 24 and 38Zn) were followed over 120 min in borate solutions of pH 9.0. For comparison, open-circuit potentials of the separate alloy constituents (copper and zinc) were also traced.

The steady state potential for brass alloy containing 38Zn was reached within 15 min from electrode immersion in the borate solution while for alloy containing 24Zn it took more than 120 min to reach steady state. Brass containing 5.5Zn shows continuous shift of the open-circuit potential towards less negative direction indicating continuous passivation over the period of measurement. Increase in the zinc content in the alloy shifts its steady state potential towards negatively, E_{ss}(Cu–5.5Zn) = −40 mV, E_{ss}(Cu–24Zn) = −120 mV, and E_{ss}(Cu–38Zn) = −180 mV, that is, toward the steady state potential of Zn.

3.1.2. *Potentiodynamic and EIS measurements*

Cyclic voltammograms for copper, zinc, and brasses with different Zn content were recorded at a scan rate of 10 mV s^{-1} in borate solution of pH 9.0. A typical cyclic voltammogram for zinc in naturally aerated borate solution at 25 °C is shown in Figure 1(a). On the anodic sweep, oxidation commenced at about −1.3 V followed by active anodic dissolution up to −1.2 V. It is reported that the predominant soluble zinc species in concentrated alkaline solutions is the tetrahedral ion [20], $Zn(OH)_4^{2-}$, but at pH 9.0, the predominant species are predicted to $Zn(OH)^+_{(aq)}$ and $Zn(OH)_{2(aq)}$ [21].

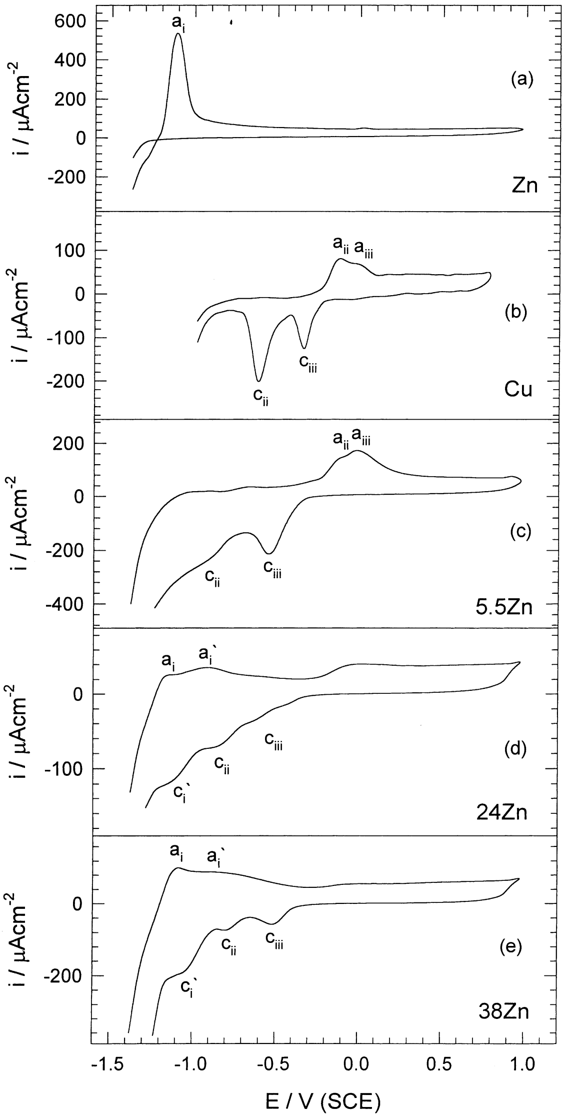

Fig. 1. Cyclic voltammograms at 10 mV s^{-1}; (a) Zn, (b) Cu, (c) Cu–5.5Zn, (d) Cu–24Zn, (e) Cu–38Zn, borate solution, pH 9.0, at 25 °C.

Therefore, the overall anodic dissolution reactions can be represented as

$$Zn + H_2O = Zn(OH)^+_{(aq)} + H^+ + 2\,e^- \tag{1a}$$

$$Zn + 2\,H_2O = Zn(OH)_{2(aq)} + 2\,H^+ + 2\,e^- \tag{1b}$$

When the electrolyte in the immediate vicinity of the electrode becomes supersaturated with zincate, porous $Zn(OH)_2$ precipitates on the surface leading to the formation of the passive film of ZnO (a_i) at about −1.1 V [21]. Once the passive film ZnO (or hydrated oxide $Zn(OH)_2$) is formed, the anodic dissolution is inhibited and the anodic current reduced significantly to low values. The reverse potential scan does not show a clear cathodic peak corresponding to the reduction of the passive film. This can be attributed to the overlap of the reduction of dissolved oxygen and passive film just preceding the potential range of the hydrogen evolution reaction [22].

A cyclic voltammogram for copper in naturally aerated borate solution at 25 °C is shown in Figure 1(b). Soon after commencing the potential scan at −1.0 V vs SCE, low cathodic current is observed probably due to the formation of adsorbed species such as $Cu(H_2O)_{ads}$ and/or $Cu(OH)^-_{ads}$ at the electrode surface [23, 24] namely:

$$Cu + H_2O = Cu(H_2O)_{ads} \tag{2a}$$

$$Cu + OH^- = Cu(OH)^-_{ads} \tag{2b}$$

This adsorbed layer inhibits the hydrogen evolution reaction leading to the observed low cathodic current. Then two anodic peaks are observed at −0.15 V (a_{ii}) and 0.0 V (a_{iii}) (cf. Figure 1(b)). The anodic peak (a_{ii}) can be attributed to a combination of a dissolution–passivation processes described as follows:

(a) *Dissolution*. That is, the dissolution of the adsorbed layer according to

$$Cu(OH)^-_{ads} + OH^- = Cu(OH)^-_{2(aq)} + e^- \tag{3a}$$

$$Cu(H_2O)_{ads} + OH^- = Cu(OH)^-_{2(aq)} + H^+ + e^- \tag{3b}$$

(b) *Passivation*. That is, formation of a passive film of Cu_2O [25], according to

$$2Cu(OH)^-_{2(aq)} = Cu_2O + H_2O + 2\,OH^- \tag{3c}$$

$$2Cu(OH)^-_{(ads)} = Cu_2O + H_2O + 2\,e^- \tag{3d}$$

The anodic peak (a_{iii}) can be attributed to the conversion of the outer layer of the oxide film, Cu_2O, at the oxide–solution interface to Cu(I)/Cu(II) oxide or a hydrated oxide [25], according to

$$Cu_2O + H_2O = 2\,CuO + 2\,H^+ + 2\,e^- \tag{4a}$$

$$Cu_2O + 3\,H_2O = 2\,Cu(OH)_2 + 2\,H^+ + 2\,e^- \tag{4b}$$

The potential scan in the negative direction shows two cathodic peaks at −0.35 V (c_{iii}) and −0.6 V (c_{ii}). The cathodic peak (c_{iii}) is attributed to the electroreduction of $Cu(OH)_2$ while peak (c_{ii}) is related to the electroreduction of Cu_2O [25].

Cyclic voltammograms for brasses containing 5.5, 24 and 38Zn in borate solution are shown in Figure 1 ((c), (d) and (e)). On the anodic sweep for Cu–5.5Zn (c.f. Figure 1 (c)), oxidation commences at about −1.1 V showing low anodic current with no clear anodic peak up to −0.24 V. This means that the ZnO formed with no significant dissolution due to low zinc content in this alloy. The cyclic voltammogram exhibits ill-defined anodic peak (a_{ii}) at about −0.15 V and another anodic peak (a_{iii}) at 0.0 V, which can be attributed to the formation of Cu(I) and Cu(II), respectively. The reverse potential scan shows two cathodic peaks at −0.55 V (c_{iii}) and −0.95 V (c_{ii}) corresponding to the reduction of Cu(II) to Cu(I) and Cu(I) to Cu, respectively [13].

On the anodic sweep for Cu–24Zn and Cu–38Zn (cf. Figure 1(d) and (e)), oxidation commenced at about −1.2 V. The cyclic voltammogram exhibits a shoulder (a_i) for Cu–24Zn or an ill-defined anodic peak at about −1.15 V for Cu–38Zn, which can be attributed to the formation of ZnO. A hump (a'_i) was observed at about −0.9 V which can be attributed to zinc dissolution through the passive layer and a concomitant growth of a passive layer on zinc [13]. The anodic peak at 0.0 V which believed to be due to formation of Cu(II) oxide was appeared as a shoulder for Cu–24Zn and almost vanished for Cu–38Zn. It seems that the presence of zinc reduces the dissolution of copper due to the formation of a compact passive film of ZnO at the electrode surface. The potential scan in the negative direction shows three cathodic peaks at about −0.55 V (c_{iii}) and −0.8 V (c_{ii}) related to the reduction of Cu(II) and Cu(I). The third cathodic peak (c'_i)–1.05 V can be attributed to the reduction of ZnO and soluble species (Zn(II)) produced in the preceding half cycle [13].

To evaluate the effect of the alloying on the corrosion process taking place at the brass–electrolyte interface, the effect of various zinc content was investigated in borate solution. Using potentiodynamic Tafel polarization data the values of the corrosion current density, i_{corr}, and corrosion potential, E_{corr}, were calculated and are presented in Figure 2. The corrosion current density, i_{corr}, decreases exponentially with increasing Zn content. Also, increase in zinc content shifts the corrosion potential towards more negative values. that is, towards the corrosion potential of Zn.

The impedance data recorded after 120 min of electrode immersion in borate solutions of pH 9.0 are presented in Figure 3. The Bode plots of three alloys with different Zn content (5.5, 24, 38) show only one phase maximum at intermediate frequencies and 45° phase shift at low frequencies. The presence of one phase maximum indicates the presence of only one time constant corresponding to the impedance of the spontaneously formed passive film. The absence of the impedance plateau and the presence of 45° phase shift at low frequencies indicate the presence of diffusion process in the solution at the electrode surface. The impedance values of different brasses in borate solution were found to depend on Zn content (c.f. Figure 3).

The impedance data for brasses were analysed using software provided with the impedance system. The equivalent circuit model consists of a capacitor, C, in parallel with a resistor, R_p, representing the passive film capacitance and resistance, respectively, and the solution resistance is represented by a resistor, R_s, in series with the above parallel combination. The electrode impedance of this combination, Z, is represented by

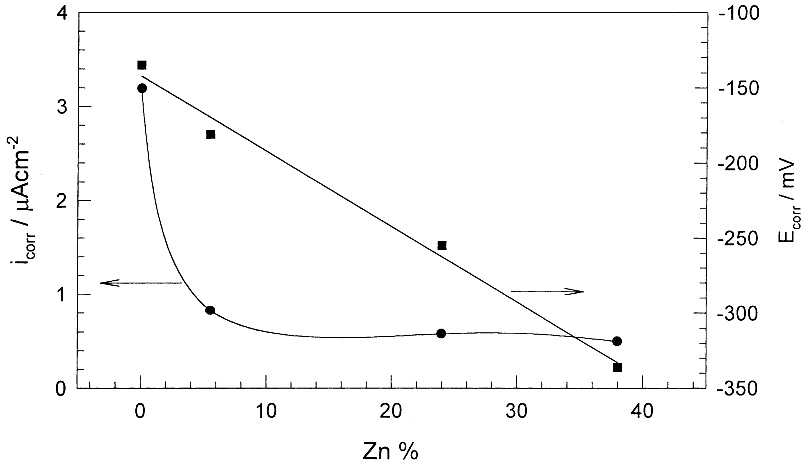

Fig. 2. Corrosion current and corrosion potential of Cu–Zn alloys in borate solution, pH 9.0, as a function of Zn content.

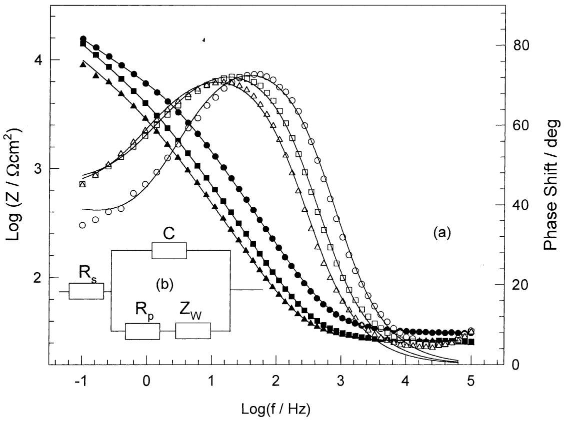

Fig. 3. (a) Bode plots of Cu–Zn alloys after 120 min of immersion in borate solution, pH 9.0, at 25 °C. (b) Equivalent circuit used in the fitting of the impedance data of Cu–Zn alloys at different conditions. R_s = solution resistance, R_p = passive film resistance, C = passive film capacitance, and Z_w = Warburg impedance. Key: (●) Cu–5.5Zn; (■) Cu–24Zn; (▲) Cu–38Zn; (— —)simulated data.

Table 1. Equivalent circuit parameters for brasses with different Zn content after 120 min of electrode immersion in borate solution of pH 9.0 at 25 °C

Zn/%	R_s/Ω	C/μF cm^{-2}	α	R_p/kΩ cm^2	W/kΩ s$^{-1/2}$
0	140	7.8	0.83	3.1	11.3
5.5	153	4.6	0.86	10.4	34.2
24	144	8.3	0.86	23.5	26.7
38	176	11.2	0.86	21.4	20.3

$$Z = R_s + \frac{R_p}{1 + (2\pi f R_p C)^{\alpha}} \tag{5}$$

where α denotes an empirical parameter ($0 \le \alpha \le 1$) and f is the frequency in Hz. The above relation is known as the dispersion formula and takes into account the deviation from the ideal RC-behaviour in terms of a distribution of time constants due to surface inhomogeneities, roughness effects, and variations in properties or compositions of surface layers [22, 26, 27]. The impedance of alloys with different zinc content were analysed using the equivalent circuit shown in Figure 3(b) where a Warburg impedance, Z_w, was introduced to account for a diffusion process within the interfacial layer of the solution. Such diffusion process may indicate a reversible dissolution process, that is, the passive film formation under open-circuit conditions proceed through a dissolution-precipitation mechanism [19, 28]. The calculated equivalent circuit parameters for brasses with different Zn content are presented in Table 1. The passive film shows some degree of heterogeneity ($\alpha = 0.86$). The passive film resistance, R_p, increases with the increase in Zn content (cf. Figure 4).

The passive film thickness is given by:

$$d = \frac{\varepsilon \varepsilon_o}{C} \tag{6}$$

where d is the film thickness, ε the dielectric constant of the passive film, ε_o the permittivity of free space 8.85×10^{-14} F cm^{-1} and C is the capacitance of the passive film. Although the actual value of ε within the film is difficult to estimate, a change of C can be used as an indicator of a change in the film thickness, d. The reciprocal capacitance of the passive film, $1/C$, is directly

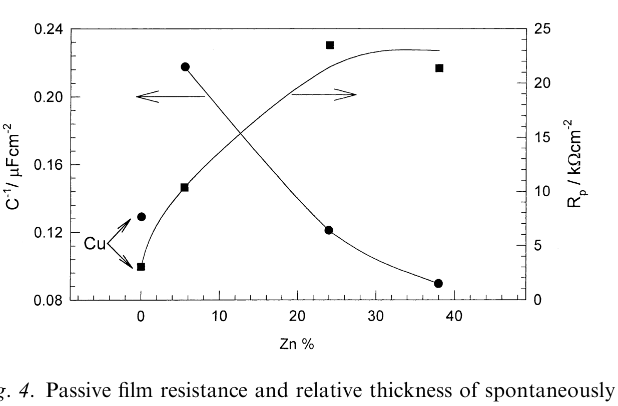

Fig. 4. Passive film resistance and relative thickness of spontaneously formed film on Cu–Zn alloys in borate solution, pH 9.0, as function of Zn content.

proportional to the thickness of the passive film. The values of $1/C$ show an increase for Cu–5.5Zn brass followed by a continuous decrease with increasing of alloying Zn (cf. Figure 4). This indicates that a thin compact film is formed for high Zn content alloys (24 and 38 Zn).

3.2. *Effect of Pb as a minor alloying element*

Lead is virtually insoluble in the α-brasses and, when present, occurs as finely divided and distributed metallic particles. It is believed that β-phase can hold up to 1% of lead in solution. The lead is added to brass to improve its machinability [18]. However, some work on corrosion behaviour of leaded brasses is reported [11, 12].

3.2.1. *Open-circuit potential measurements*

Open-circuit potentials of brass (Cu–38Zn) with different Pb content (1.4, 2.7 and 3.3Pb) were recorded over 120 min in borate solutions of pH 9.0. The steady state potential for brass alloy containing no Pb was reached within 15 min from electrode immersion in the borate solution while the brass containing 3.3Pb it took more than 60 min to reach steady state. For leaded brasses containing 1.4 or 2.7Pb a continuous shift of the open-circuit potential in the less negative direction was recorded, which indicates continuous passivation over the period of measurement.

3.2.2. *Potentiodynamic and EIS measurements*

The cyclic voltammograms of Cu–38Zn and its leaded alloys were recorded at a scan rate of 10 mV s^{-1} in borate solutions of pH 9.0. There is no significant effect of the Pb addition on the general features of the cyclic voltammograms of Cu–38Zn alloy.

The effect of addition of Pb to the Cu–38Zn brass was studied in borate solution using the polarization technique. The values of the i_{corr}, and E_{corr} were calculated and are presented in Figure 5. The corrosion current, i_{corr}, of leaded brass (2.7 and 3.3 Pb) was found to be comparable with that of unleaded brass.

The impedance data recorded after 120 min of electrode immersion in borate solutions are presented in Figure 6. The Bode plots of the three leaded brasses with different Pb content show similar characteristics to those observed for unleaded brasses. The impedance values were found to increase with increasing Pb content.

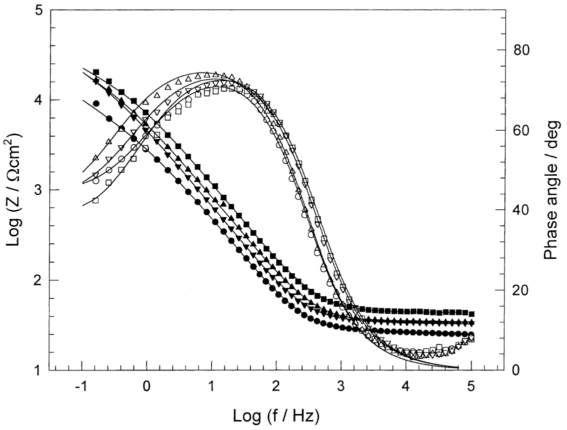

Fig. 6. Bode plots of leaded Cu–38Zn alloy after 120 min of immersion in borate solution, pH 9.0, at 25 °C. Key: (●) Cu–38Zn–0.0Pb; (■) Cu–38Zn–1.4Pb; (▲) Cu–38Zn–2.7Pb; (▼) Cu–38Zn–3.3Pb; (— —) simulated data.

The impedance data for Cu–38Zn alloy with different Pb content (1.4–3.3Pb) in borate solution under open-circuit potential conditions were analysed using the same equivalent circuit model described above (cf. Figure 3(b)). The calculated equivalent circuit parameters are presented in Table 2. The passive film resistance, R_p, increases with the increase in Pb content (cf. Figure 7). This means that the addition of Pb to

Table 2. Equivalent circuit parameters for brasses with different Pb content after 120 min of electrode immersion in borate solution of pH 9.0 at 25 °C

Pb/%	R_s/Ω	$C/\mu F\ cm^{-2}$	α	$R_p/k\Omega\ cm^2$	$W/k\Omega\ s^{-1/2}$
0.0	176	11.2	0.86	21.4	20.3
1.4	202	7.2	0.85	21.4	45.9
2.7	170	7.8	0.85	26.4	45.6
3.3	167	10.1	0.86	37.7	44.4

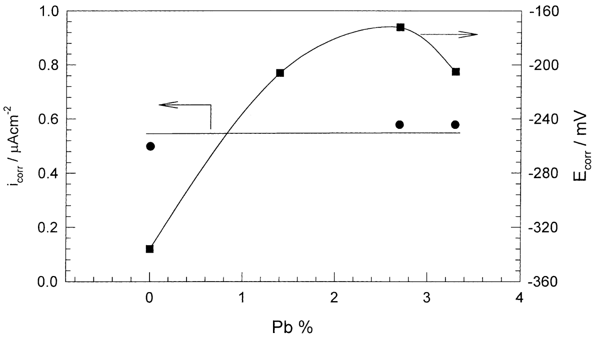

Fig. 5. Corrosion current and corrosion potential of leaded Cu–38Zn alloy in borate solution, pH 9.0, as a function of the Pb content.

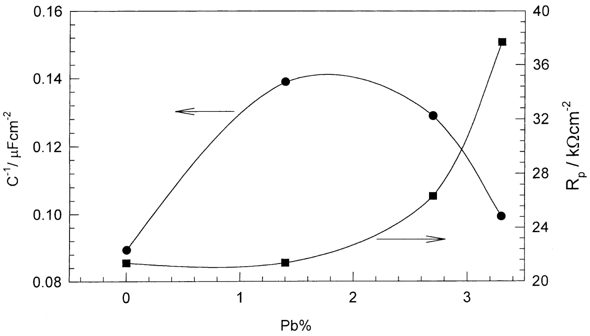

Fig. 7. Passive film resistance and relative thickness of spontaneously formed film on leaded Cu–38Zn alloy in borate solution as a function of Pb content.

brass not only improves it machinability but also its corrosion stability. This improvement in the corrosion stability of leaded brass can be attributed to the formation of a stable passive film. The values of $1/C$ shows a similar behaviour to those obtained with brasses containing different zinc content, where the passive film thickness increases with addition of Pb then decreases with increasing Pb content (cf. Figure 7).

3.3. *Potentiostatic film formation and EIS measurements*

A constant potential was applied to the Cu–38Zn alloy in borate solution until a steady state was reached and then the impedance spectra were recorded. The results of these measurements are presented as Bode plots in Figure 8. The impedance measurements at different potentials were analysed using the equivalent circuit shown in Figure 3(b). The calculated equivalent circuit parameters at different potentials are presented in Table 3. The presence of a diffusion contribution may indicate that the passive film formation under potentiostatic condition proceeds through a dissolution–precipitation mechanism [19, 28]. The impedance measurements show passivation behaviour for applied potentials form −1.2 to +0.6 V, where the passive film formed on the alloy shows considerably high resistance range from 0.7 to 106 kΩ cm^2. For an applied potential ≥+0.6 V the calculated passive film resistance decreases to lower values. For example the passive film resistance decreases form 106 kΩ cm^2 at +0.6 V to 42 kΩ cm^2 at +0.8 V indicating an anodic dissolution at this potential.

Table 3. Equivalent circuit parameters for Cu–38Zn electrode in borate solution of pH 9.0 at different applied potentials at 25 °C

E_{app}/mV	R_s/Ω	C/μF cm^{-2}	α	R_p/kΩ cm^2	W/kΩ s$^{-1/2}$
−1200	155	96.9	0.87	0.7	4.5
−1100	154	33.1	0.87	1.2	8.5
−1050	156	36.4	0.86	1.5	10.6
−1000	156	25.3	0.89	1.5	12.5
−800	152	20.2	0.87	2.6	16.1
−400	155	26.6	0.87	3.9	22.7
0	156	5.2	0.87	23.8	49.5
200	157	4.9	0.87	64.3	83.2
400	154	3.9	0.87	108.3	77.5
600	332	2.9	0.85	106.3	118.2
800	326	4.7	0.85	42.4	145.4

Figure 9 shows linear variations of the passive film resistance, R_p, and the relative passive film thickness, $1/C$, with applied potential. A break point in the linear variation of the passive film resistance, and the relative passive film thickness, $1/C$, was observed at about −0.2 V. At applied potentials >−0.2 V the growth rate of the passive film is higher than that at lower potentials. This change in the growth rate of the passive film during anodization indicates a change in the passive film structure. At a potential −1.2 V and higher, ZnO is formed and its thickness increases linearly with increasing the applied potential [21]. This means that the passive film formed on the brass alloy at potentials lower than −0.2 V consists mainly of ZnO. At higher applied potentials (>−0.2 V), in addition to the continuous increase in the passive film thickness of zinc, the formation and the increase in the passive film thickness of copper oxides with potential are expected. It is always expected that copper alloys containing more active metals (e.g., Zn), the alloying element will appear as an

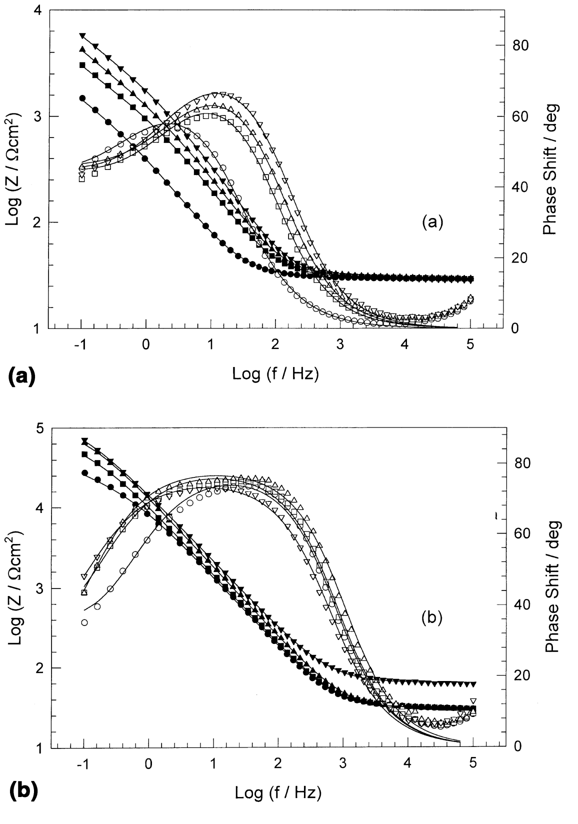

Fig. 8. Bode plots of Cu–38Zn alloy in borate solution, pH 9.0, at different applied potentials. (a): (●) −1.2 V, (■) −1.1 V, (▲) −1.0 V, (▼) −0.8 V, and (——) simulated data; (b): (●) 0.0 V, (■) 0.2 V, (▲) 0.4 V, (▼) 0.6 V, and (——) simulated data.

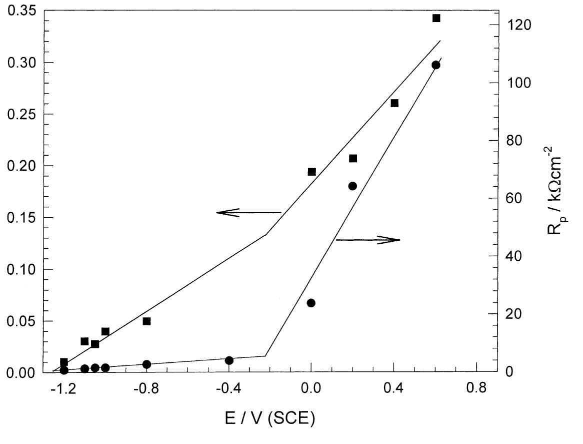

Fig. 9. Passive film resistance and relative thickness of surface film formed on Cu–38Zn alloy in borate solution, pH 9.0, as a function of applied potential.

oxide in the passive film, often in greater concentration than in the alloy itself, and sometimes to the exclusion of copper oxides [17]. The passive film resistance shows the same trend as the passive film thickness. This means that passive film consisting of Zn and Cu oxides is thicker and more protective than that consisting of zinc oxide only.

3.5. *Effect of chloride ions on the electrochemical behaviour of brass*

The effect of addition chloride ions with various concentrations (0.01–0.6 M) on the electrochemical behaviour of brass (Cu–38Zn) in borate solution was investigated using potentiodynamic technique at a scan rate 1 mV s^{-1}. Addition of 0.01 M Cl^- shifts the corrosion potential to less negative then the increase in the Cl^- ions concentration shifts the corrosion potential to more negative values. The presence of 0.01 M Cl^-, in borate solution, increases the corrosion current by one order of magnitude. Then the corrosion current was found to decrease with increasing the chloride ion concentration up to 0.2 M Cl^-. For concentrations higher than 0.2 M Cl^- an increase in the corrosion current was observed. It seems that the presence of low concentration of Cl^- ions (0.01 M) leads to significant dissolution of Zn leaving Cu at the surface of the alloy. Then the continuous decrease in the corrosion current with increasing the chloride ion concentration is due to the formation of an insoluble film consists mainly of CuCl [23]. Above a critical concentration (> 0.2 M), Cl^- ions attacks the insoluble layer of CuCl to form soluble complex of $CuCl_2^-$ leading to the observed increase in the corrosion rate.

The corrosion current density of the Cu–38Zn alloy was found to change exponentially with chloride ion concentration. This means that $\log i_{corr}$ is a linear function of the concentrations of Cl^- (cf. Figure 10). This linear relation for each segment can be formulated mathematically as

$$\log i_{corr} = \log k + \alpha[Cl^-] \qquad (7)$$

Where k is a constant which can be obtained from the intercept of the linear, $\log i_{corr}$ against $[Cl^-]$ relation and α is its slope, $d \log i_{corr}/d[Cl^-]$. The break point in the above relation can be considered as the chloride ion concentration at which the insoluble layer of CuCl is attacked by Cl^- to form soluble complex $CuCl_2^-$.

The i/E curves exhibit an abrupt increase in the anodic current when a critical potential value (E_b) is exceeded. The current increases at potentials greater than E_b is associated with pitting corrosion and film breakdown. Values of E_b for the Cu–38Zn alloy were determined from anodic polarization curves recorded from −0.4 V upward at a scan rate 1 mV s^{-1} in the borate solution containing Cl^- ions (0.01–0.6 M). The increase in the Cl^- ion concentration shifts E_b towards less positive values. It was found that the E_b varies linearly with the logarithm of chloride ion concentration (cf. Figure 11) according to the following relation [29]:

$$E_b = a - b \log[Cl^-] \qquad (8)$$

where a and b are constants whose values depend on the scan rate [23].

4. Conclusions

(i) The corrosion rate of brass in borate solution decreases with increasing zinc content.
(ii) The corrosion rates of leaded brasses are comparable with those of unleaded brass.
(iii) Long immersion of different brasses improves their corrosion resistance due to the spontaneously formed passive film.
(iv) The passive film formation under different conditions is believed to proceed through a dissolution–precipitation mechanism.
(v) Increase in chloride ions concentration decreases the corrosion rate of brass due to the formation of insoluble CuCl up to a critical chloride ion concentration when the corrosion rate increases due to the formation of soluble $CuCl_2^-$ complex.

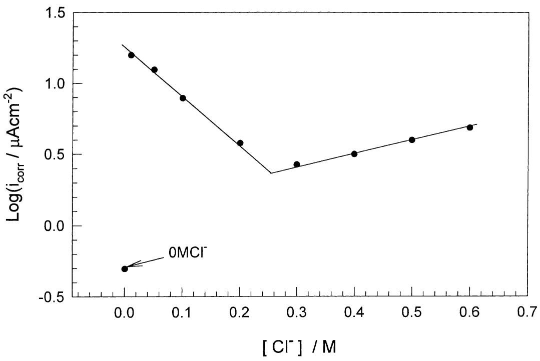

Fig. 10. Variation of the rate corrosion of Cu–38Zn alloy in borate solution, pH 9.0, as a function of Cl^- ion concentrations at 25 °C.

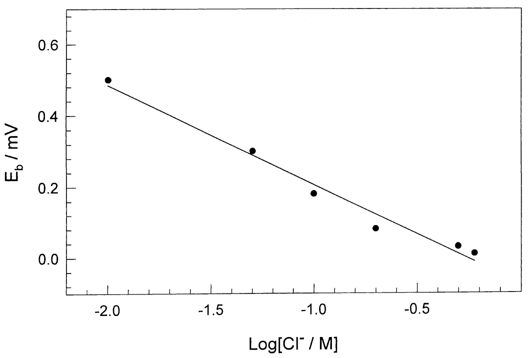

Fig. 11. Variation of E_b of Cu–38Zn alloy in borate solution containing Cl^- ion, pH 9.0, as a function of log Cl^- ion concentrations at 25 °C.

References

1. J. Sugawra and H. Ebike, *Corros. Sci.* **7** (1967) 513.
2. G. Joseph and M.T. Arce, *Corros. Sci.* **7** (1967) 597.
3. H.W. Pickering and P.J. Byrne, *J. Electrochem. Soc.* **116** (1969) 1492.
4. H.W. Pickering, *J. Electrochem. Soc.* **117** (1970) 8.
5. A.H. Taylor, *J. Electrochem. Soc.* **118** (1971) 854.
6. J.E. Holliday and H.W. Pickering, *J. Electrochem. Soc.* **120** (1973) 470.
7. A.M. Shams El-Din and F.M. Abd-El-Wahab, *Corros. Sci.* **17** (1977) 49.
8. J.E. Ennegar, R.E. Hummel and E.D. Verink, *Corrosion* **37** (1981) 256.
9. M.J. Proyer and J.C. Fister, *J. Electrochem. Soc.* **131** (1984) 1230.
10. R.K. Dinnappa, and S.M. Mayanna, *Corros. Sci.* **27** (1987) 349.
11. W.A. Badawy, S.S. El-Egamy and A.S. El-Azab, *Corros. Sci.* **37** (1995) 1969.
12. S.S. El-Egamy, A.S. El-Azab and W.A. Badawy, *Corrosion* **50** (1994) 468.
13. J. Morals, G.T. Fernandez, P. Esparza, S. Gonzalez, R.C. Salvarezza and A.J. Arvia, *Corros. Sci.* **37** (1995) 211.
14. J. Morals, P. Esparza, G.T. Fernandez, S. Gonzalez, J.E. Garcia, J. Caceres, R.C. Salvarezza and A.J. Arvia, *Corros. Sci.* **37** (1995) 231.
15. B.-S. Kim, T. Piao, S.N. Hoier, and S.-M. Park, *Corros. Sci.* **37** (1995) 557.
16. A.M. Beccarria, G. Poggi and G. Capannelli, *Corros. Prevent. & Control* **86** (1989) 169.
17. P.T. Gilbert, *in* L.L. Shreir, R.A. Jarman and G.T. Burstein (Eds) 'Corrosion', 3rd edn (Butterworth–Heinemann, Oxford, repr. 1995), pp. 4:52, 4:60, 17:23 and 17:84.
18. R.A. Wilkins and E.S. Bunn, 'Copper and Copper Base Alloys', 1st edn (McGraw-Hill, 1943), pp. 29 and 89.
19. K.M. Ismail and W.A. Badawy, *J. Appl. Electrochem.*, in press.
20. R.D. Armstrong and M.F. Bell, 'Specialist Periodical Report: Electrochemistry', Vol. 4, The Chemical Society, London (1974), chapter 1.
21. D.D. Macdonald, K.M. Ismail and E. Sikora, *J. Electrochem. Soc.* **145** (1998) 3141.
22. A.E. Bohe, J.R. Vilche, K. Juettner, W.J. Lorenz and W. Paatsch, *Electrochim. Acta* **34** (1989) 1443.
23. M.R.G. De Chialvo, R.C. Salvarezza, D. Vasquez Moll and A.J. Arvia, *Electrochim. Acta* **30** (1985) 1501.
24. F.M. El-Kharafi and Y.A. El-Tantawy, *Corros. Sci.* **22** (1982) 1.
25. H.H. Strehblow and B. Titze, *Electrochem. Acta* **25** (1980) 839.
26. K. Hladky, L.M. Calow and J.L. Dawson, *Br. Corr. J.* **15** (1980) 20.
27. J. Hitzig, J. Titz, K. Juettner, W.J. Lorenz and E. Schmidt, *Electrochim. Acta* **29** (1984) 287.
28. R.D. Armstrong, *Corros. Sci.* **11** (1971) 693.
29. H.P. Lekie and H.H. Uhlig, *J. Electrochem. Soc.* **108** (1961) 209.